APS physics

CHORUS

This is the accepted manuscript made available via CHORUS. The article has been published as:

Photonic Nonlinearities via Quantum Zeno Blockade

Yu-Zhu Sun, Yu-Ping Huang, and Prem Kumar

Phys. Rev. Lett. **110**, 223901 — Published 28 May 2013

DOI: 10.1103/PhysRevLett.110.223901

Photonic Nonlinearities via Quantum Zeno Blockade

Yu-Zhu Sun,[1] Yu-Ping Huang,[2,*] and Prem Kumar[1,2]

[1] *Center for Photonic Communication and Computing and Department of Physics and Astronomy, Northwestern University, 2145 Sheridan Road, Evanston, Illinois 60208-3112, USA*

[2] *Center for Photonic Communication and Computing and Department of Electrical Engineering and Computer Science, Northwestern University, 2145 Sheridan Road, Evanston, Illinois, 60208-3118, USA*

Realizing optical-nonlinear effects at a single-photon level is a highly desirable but also extremely challenging task, because of both fundamental and practical difficulties. We present an avenue to surmounting these difficulties by exploiting quantum Zeno blockade in nonlinear optical systems. Considering specifically a lithium-niobate microresonator, we find that a deterministic phase gate can be realized between single photons with near-unity fidelity. Supported by established techniques for fabricating and operating such devices, our approach can provide an enabling tool for all-optical applications in both classical and quantum domains.

PACS numbers: 42.65.Pc, 03.65.Xp, 42.50.Ex

First observed more than half a century ago [1], optical nonlinear phenomena have since become the foundation for interdisciplinary applications, such as squeezed light sources [2], biological microscopy [3], and entanglement generation [4]. Recently, the quest for information processing by all-optical means has fueled new studies of optical phenomena in an extreme quantum regime involving only a few photons [5, 6]. This requires optical nonlinearities that are orders of magnitude higher than those achievable with existing optical media [7, 8]. Although this drawback can be overcome by combining strong cavity enhancement with resonant coupling between photons and (effective) atoms [9, 10], the implementation requires large setups and operation in near-zero-temperature environment, making such systems unsuitable for practical use. In contrast, schemes based on post selection [11] or feed forward [12] can be implemented with only linear-optics instruments. Such schemes, however, are inherently probabilistic and thus their use is hard to justify in large-scale applications.

Highly off-resonant optical nonlinearities, on the other hand, do not suffer from the aforementioned issues and are thus potentially viable for photonic information processing tasks on a large scale. It was suggested that intense cross-phase modulation (XPM) in Kerr-nonlinear media could produce a deterministic phase gate between single photons [13–15] . This idea, unfortunately, was developed upon an incorrect single-mode argument. By taking into account the inherent multimode nature of light propagation in a Kerr medium, it was recently discovered that no useful XPM effect can be produced in such systems even with an unrealistically giant Kerr nonlinearity [16, 17]. The fundamental reason turns out to be that causality prohibits XPM phase shift of any non-negligible amount without significant quantum noise.

It remains an outstanding challenge—not only because of implementation difficulties but also due to the fundamental restrictions—to construct practical nonlinear optical devices suitable for operation at the single photon level. In this Letter, we propose to surmount this challenge by exploiting the quantum Zeno effect that occurs when a slowly-evolving system is probed frequently or continuously, with the result that the system is "frozen" in its initial state (i.e., its evolution is slowed down) [18]. Applying this effect to a nonlinear optical cavity, quantum Zeno blockade (QZB) can be realized whereby occupation of a cavity mode "blocks" (more precisely, suppresses) additional photons from entering the cavity [19–21]. In effect, the intracavity photon acts as a continuous probe monitoring the in-coupling of additional photons, thereby preventing them from entering the cavity through the Zeno effect. QZB is analogous in functionality to "photon blockade" that is realized through vacuum Rabi splitting [9]. QZB instead occurs through the Zeno effect, which allows for distinct "interaction-free" operations that can potentially lead to ultralow-loss and noise-free devices for all-optical processing [21, 22].

We employ QZB to realize strong, interaction-free nonlinear effects between single photons. Specifically by considering a $\chi^{(2)}$ system of a prism-coupled lithium-niobate (LN) microdisk resonator, we show that strong XPM effects can be produced between single photons under realizable parameter settings. When the input single photons are in the form of Gaussian pulses, they become entangled at the output. However, when the input photons are prepared in exponential waveforms that are time-reversed replicas of the cavity leakage modes [23], a deterministic phase gate can be realized. This result highlights a potentially enabling pathway for implementing practical photonic information processing. Our approach is generally extendable to a variety of nonlinear optical systems of traveling-wave or resonator designs.

In Fig. 1, we schematize the operation of our phase gate. It consists of a LN microdisk cavity evanescently coupled to a prism. The cavity is designed to be in resonance with both the pump (control) and the signal (target), and the disk is quasi phase-matched to support sum-frequency generation (SFG) between the two. Fig-

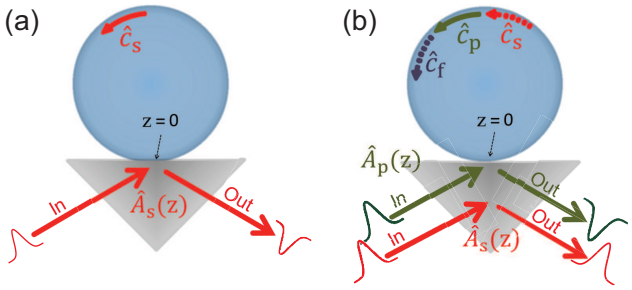

FIG. 1. A schematic of the gate setup with pump OFF (a) and ON (b). $\hat{A}_{s(p)}$ is the annihilation operator for the propagating signal (pump) field. $\hat{c}_{s(p,f)}$ is the annihilation operator for the intracavity signal (pump, sum-frequency) field. Dashed arrows indicate the interaction-free nature of the gate's operation.

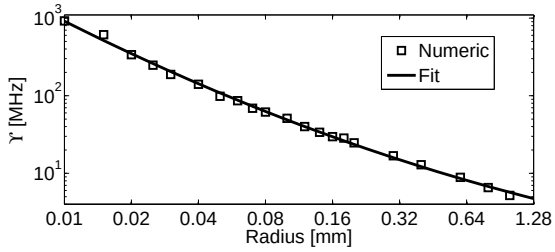

FIG. 2. Υ versus R on a log scale. The plotted curve is $\log_{10}\Upsilon = 0.073(\log_{10} R)^2 - 0.77\log_{10} R + 1.74$, which is obtained by least-square fitting.

ure 1(a) shows the pump-OFF case. Through the prism, the signal field evanescently couples into the disk and then exits with a π phase shift relative to its input. Figure 1(b) shows the pump-ON case. The pump field, applied ahead of the signal, couples in and then out of the disk with a π phase shift. When the signal photon arrives, the presence of the intracavity pump field and the large nonlinear coupling strength provide high potential for SFG. Depending on the lifetime of the sum-frequency (SF) field in the cavity, gate operation falls into two categories: incoherent quantum zeno (IQZ) and coherent quantum zeno (CQZ) [24]. IQZ corresponds to the system being monitored by a real detector or an effective one realized through dissipative coupling to a reservoir system containing many degrees of freedom [19, 25]. Our system is in IQZ when the cavity SF field is short lived, since the SFG process then causes the intracavity signal field to dissipate, thus mimicking continuous monitoring of the intracavity signal field [22]. As a result, the signal's coupling into the cavity will be suppressed through the Zeno effect. When the dissipation is strong, the incoming signal will be reflected from the cavity with its phase unchanged. In contrast, CQZ corresponds to the system being coupled to a few or just a single degree of freedom with low loss [20]. Such is the case for our system when the SF field in the cavity is long lived. The probe for the intracavity signal field is then realized through its Rabi coupling with the SF field [24]. In analogy with Autler-Townes splitting for atomic transitions [26], the intracavity pump field creates dressed states for the intracavity signal and SF fields shifting their resonant frequencies. Therefore, when CQZ is in force, similar to the IQZ case, the input signal will be reflected without changing its phase because of the shift in the resonance frequency. Below we consider the CQZ case in detail; see the supplementary material for the IQZ case.

The eigenmodes of the microdisk cavity are whispering gallery modes (WGMs). See details in the supplementary material [27]. For a typical LN microdisk with radius $R \simeq 1.5$ mm and $Q^{\rm i} > 10^7$ [28], the resonance linewidth is much smaller than the cavity's free-spectral range. It is thus valid to consider only a single cavity mode being excited by the corresponding applied external quasimonochromatic field. We then denote the cavity-mode annihilation operators as $\hat{c}_\mu$ with $\mu \in \{\mathrm{s,p,f}\}$ representing the signal, pump, and SF fields, respectively. They satisfy $[\hat{c}_\mu, \hat{c}^\dagger_{\mu'}] = \delta_{\mu\mu'}$ and $[\hat{c}_\mu, \hat{c}_{\mu'}] = 0$. The corresponding external propogating-field annihilation operators are denoted by $\hat{A}_\mu$, which satisfy $[\hat{A}_\mu(z), \hat{A}^\dagger_{\mu'}(z')] = \delta_{\mu\mu'}\delta(z-z')$ and $[\hat{A}_\mu(z), \hat{A}_{\mu'}(z')] = 0$.

To capture the temporal behavior of pulsed optical signals, a temporally multimode quantum description is needed. We consider an effective real-space Hamiltonian specific to our gate system, as follows [29]:

$$\begin{aligned}\hat{H} = \sum_{\mu=\mathrm{s,p,f}} \Bigg[& \hbar\omega_\mu \hat{c}^\dagger_\mu \hat{c}_\mu + \int \mathrm{d}z\, \hat{A}^\dagger_\mu(z)\hbar(\omega_\mu - iv_{\mathrm{g}}\frac{\partial}{\partial z})\hat{A}_\mu(z) \\ & + \hbar\sqrt{v_{\mathrm{g}}\frac{\omega_\mu}{Q^{\mathrm{c}}_\mu}} \int \mathrm{d}z\, \delta(z)(\hat{A}^\dagger_\mu(z)\hat{c}_\mu + \hat{A}_\mu(z)\hat{c}^\dagger_\mu)\Bigg] \\ & + \hbar\left(\Upsilon \hat{c}_{\mathrm{s}}\hat{c}_{\mathrm{p}}\hat{c}^\dagger_{\mathrm{f}} + \Upsilon^* \hat{c}^\dagger_{\mathrm{s}}\hat{c}^\dagger_{\mathrm{p}}\hat{c}_{\mathrm{f}}\right),\end{aligned} \tag{1}$$

where ω_μ is the carrier frequency of the field $\hat{A}_\mu$ and v_{g} is the group velocity which is assumed to be the same for all the pulsed fields. Since the carrier-frequency terms in Eq. (1) do not influence the gate's dynamics, we ignore terms containing $\hbar\omega_\mu$ for simplicity. The third term in Eq. (1) describes the coupling between the external propagating fields and the cavity fields, where the coupling quality factor Q^{c}_μ places a bandwidth limit on the input pulses that can be properly coupled-in without distortion. The last two terms in Eq. (1) describe the intracavity SFG process, where Υ is the nonlinear coupling coefficient. In Fig. 2 we plot Υ as a function of R calculated using analytical WGM profiles (see supplementary material [27] for details), where $\Upsilon = 140$ and 337 MHz are shown to be obtained for $R \approx 50$ and 20 µm, respectively. Such large Υ values are potentially realizable because high-quality LN microdisks with R as small as 40 µm have been fabricated via manual polishing tech-

niques [30]. Even smaller disks are expected to be fabricated in the near future by adopting advanced automated machining and polishing.

In arriving at Eq. (1), we have assumed $Q_\mu^{\rm c} \ll Q_\mu^{\rm i}$ and thus have neglected terms that describe decay of the WGMs. $Q_\mu^{\rm i}$ is fundamentally limited by bending loss and light absorption within the disk. Because LN's large refractive index, the bending loss allows for $Q_\mu^{\rm i} > 10^{14}$ for disks with $R > 15\,\mu$m [31, 32]. On the other hand, the absorption loss in commercially-available LN crystals is usually $\sim 10^{-4}$/cm or higher, which imposes a high limit of $Q_\mu^{\rm i} \sim 10^8$, as typically demonstrated [33]. By custom doping LN crystals, however, ultralow absorption loss ($\lesssim 10^{-5}$ cm^{-1}, bounded by measurement precision) has been demonstrated over a wide spectral range (800–2000 nm) [34]. Using such crystals, microdisks with $Q_\mu^{\rm i} \gtrsim 10^9$ can be fabricated. Note that in practice $Q_\mu^{\rm i}$ can also be limited by roughness of the disk's surface. This effect, however, was not found to be significant, even for a manually-polished disk with $R = 40\,\mu$m [30]. Based upon the above analysis, we will take $Q_\mu^{\rm i} = 10^9$, for which decay of the WGMs can be ignored when $Q_\mu^{\rm c} \lesssim 10^8$. For the setup depicted in Fig. 1, the latter conditions can be realized by adjusting the distance between the disk and the prism.

In our gate system, the joint quantum state of the signal, the pump, and the SF photons can be written in its most general form as: $|\Psi(t)\rangle = \Big[\iint {\rm d}z{\rm d}z' \phi_{\rm sp}(z,z',t)\hat{A}_{\rm s}^\dagger(z)\hat{A}_{\rm p}^\dagger(z') + \int {\rm d}z\, \phi_{\rm f}(z,t)\hat{A}_{\rm f}^\dagger(z) + \int {\rm d}z\, \phi_{\rm s}(z,t)\hat{A}_{\rm s}^\dagger(z)\hat{c}_{\rm p}^\dagger + \int {\rm d}z\, \phi_{\rm p}(z,t)\hat{A}_{\rm p}^\dagger(z)\hat{c}_{\rm s}^\dagger + e_{\rm sp}(t)\hat{c}_{\rm s}^\dagger\hat{c}_{\rm p}^\dagger + e_{\rm f}(t)\hat{c}_{\rm f}^\dagger\Big]|0\rangle$, where $|0\rangle$ is the vacuum state. The first term represents the state in which both the signal and the pump photons are in external traveling-wave modes with $\phi_{\rm sp}(z,z',t)$ as their joint wavefunction. Similarly, in the second term $\phi_{\rm f}(z,t)$ is the wavefunction for the external SF field. The third and fourth terms, in contrast, represent quantum states with one photon in the propagating mode and one in the cavity mode with $\phi_{\rm s}$ ($\phi_{\rm p}$) as the product of the signal (pump) wave function and the cavity excitation amplitude for the pump (signal). Finally, $e_{\rm f}$ ($e_{\rm sp}$) is the SF (product of signal and pump) cavity-excitation amplitude(s).

Plugging the Hamiltonian of Eq. (1) and the quantum state $|\Psi(t)\rangle$ into the Schrödinger equation, the following partial differential equations can be derived:

$$\partial_t\phi_{\rm f} = -v_{\rm g}\partial_z\phi_{\rm f} - i\Omega_{\rm f}\delta(z)e_{\rm f}, \quad (2a)$$

$$\partial_t\phi_{\rm sp} = -v_{\rm g}(\partial_z + \partial_{z'})\phi_{\rm sp} - i\sum_\nu \Omega_\nu\Lambda_{\nu'}, \quad (2b)$$

$$\partial_t\phi_\nu = -v_{\rm g}\partial_z\phi_\nu - i\Omega_\nu\delta(z)e_{\rm sp} - i\Omega_{\nu'}\Gamma_{0\nu}, \quad (2c)$$

$$\partial_t e_{\rm sp} = -i\sum_\nu \Omega_\nu\phi_\nu(0) - i\Upsilon^* e_{\rm f}, \quad (2d)$$

$$\partial_t e_{\rm f} = -i\Omega_{\rm f}\phi_{\rm f}(0) - i\Upsilon_{\rm sp}e_{\rm sp}, \quad (2e)$$

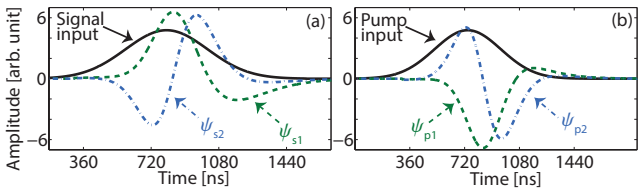

FIG. 3. Gate performance with Gaussian pump and signal pulses. (a) Signal input and the first two Schmidt eigenmodes for the signal output. (b) Pump input and the first two Schmidt eigenmodes for the pump output.

where $\Omega_\mu = (v_{\rm g}\omega_\mu/Q_\mu^{\rm c})^{1/2}$ and $\nu,\nu' \in \{{\rm s},{\rm p}\}$, $\nu \neq \nu'$. In Eq. (2b), $\Lambda_{\rm s} = \delta(z')\phi_{\rm s}(z,t)$ and $\Lambda_{\rm p} = \delta(z)\phi_{\rm p}(z',t)$. In Eq. (2c), $\Gamma_{0{\rm s}} = \phi_{\rm sp}(z,0,t)$ and $\Gamma_{0{\rm p}} = \phi_{\rm sp}(0,z',t)$. In Eq. (2), the output joint wavefunction for the signal and pump photons can be decomposed as $\phi_{\rm sp}(z,z',t) = \sum_{n=1}^\infty a_n\psi_{{\rm s}n}(z,t)\psi_{{\rm p}n}(z',t)$ $(z,z'>0)$, where $\psi_{{\rm s}n}$ and $\psi_{{\rm p}n}$ are paired mode-functions for the Schmidt modes of the output signal and pump photons, respectively, with decomposition coefficients a_n that are ordered such that $a_1 > a_2 > \cdots \geq 0$. The corresponding two-photon output state can then be written in the time domain as $|\Psi_{\rm out}\rangle = \sum_{n=1}^\infty a_n|nn\rangle$, where $|nn\rangle = v_{\rm g}^2\iint dt\,dt'\psi_{{\rm s}n}(z\to 0^+,t)\psi_{{\rm p}n}(z\to 0^+,t')\hat{A}_{\rm s}^\dagger(v_{\rm g}t)\hat{A}_{\rm p}^\dagger(v_{\rm g}t')|0\rangle$ is the $n^{\rm th}$ Schmidt-mode basis state. A near-unity a_1^2 together with a large overlap between the first Schmidt mode-function of the output signal photon and its input $\psi_{\rm s}$, as quantified by the fidelity $\left|\int dt\ \psi_{\rm s}(t)\psi_{\rm s1}^*(z\to 0^+,t)\right|^2$, then signify high-performance switching when the pump is on.

To examine the gate performance, we first consider $Q_{\rm s,p,f}^{\rm c} = 10^8$, $\Upsilon = 610$ MHz, and two 500 ns (FWHM) Gaussian signal and pump pulses with a separation of 60 ns. The simulation results are shown in Fig. 3, where the output photons turn out to be in an entangled two-photon state with $a_1 = 0.77$, $a_2 = 0.52$, $a_3 = 0.25$, and $a_{n>3} \simeq 0$. This result points to a viable approach for *on-demand* generation of time-bin entanglement (i.e., photons entangled in the temporal degree of freedom [35]) using two initially uncorrelated photons. Such photons, unlike their polarization entangled cousins, are better suited for applications in standard telecommunication fibers [35, 36] because of their insensitivity to polarization-mode decoherence occurring in such fibers.

The physics underlying the above behavior is in some way similar to what was found during the study of single-photon cross-phase modulation in the fast-response regime [16]. In a nutshell, it is because the QZB is effective only if the pump photon is in the cavity. Therefore, the phase of the signal photon can be switched only when it arrives within the cavity lifetime of the pump photon. In the above example, the cavity lifetime is about 100 ns for both the signal and pump photons, which is five times smaller than their pulse widths.

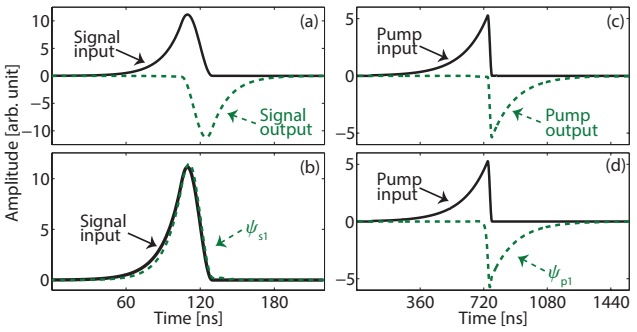

FIG. 4. CQZ gate performance with the proposed pulse shapes. Input (output) is defined as the pulse after it has evolved the same period of time without (with) passing the gate. The temporal reference points are the same in all the plots. (a) Pump OFF: the signal output is phase shifted by π and temporally reversed. (b) Pump ON: The output signal is well preserved. (c) Signal OFF: the pump behaves the same as the signal in the pump-OFF case. (d) Signal ON: the pump behaves as if there is no signal photon.

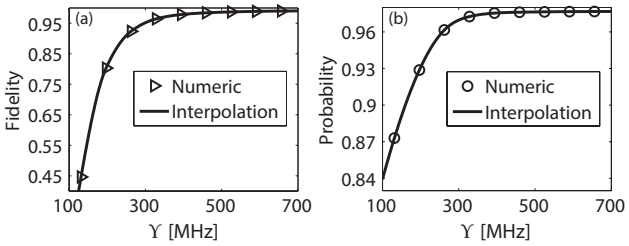

FIG. 5. Single-photon gate performance vs. nonlinear coupling strength Υ. Both the fidelity (a) and the probability of occupying the first Schmidt eigenmode (b) saturate as Υ increases.

As a result, depending on the temporal location of the pump photon within its pulse duration, the output signal photon will be in a superposition of phase changed and unchanged sates. Because of the quantum uncertainty inherent in the pump-photon location, the two photons therefore exit the cavity in an entangled state. This phenomenon can be intuitively understood by considering a toy model in which the pump and the signal photons are initially in states $(|t_0\rangle_\mathrm{p} + |t_1\rangle_\mathrm{p})/\sqrt{2}$ and $(|t_0 + \Delta\rangle_\mathrm{s} + |t_1 + \Delta\rangle_\mathrm{s})/\sqrt{2}$, respectively, where $\{|t\rangle_{\mathrm{p(s)}}\}$ are orthonormal time modes centered at t for the pump (signal). The times t_1 and Δ are chosen such that the signal photon in $|t_{0(1)} + \Delta\rangle_\mathrm{s}$ arrives at the cavity when the pump photon in $|t_{0(1)}\rangle_\mathrm{p}$ has already coupled into the cavity, but the photon in $|t_{1(0)}\rangle_\mathrm{p}$ has not (exited). Under this condition, the output pump and signal photons in the presence of an ideal QZB effect will be in an entangled state of $\big(|t_0\rangle_\mathrm{p}|t_1 + \Delta\rangle_\mathrm{s} + |t_1\rangle_\mathrm{p}|t_0 + \Delta\rangle_\mathrm{s} - |t_0\rangle_\mathrm{p}|t_0 + \Delta\rangle_\mathrm{s} - |t_1\rangle_\mathrm{p}|t_1 + \Delta\rangle_\mathrm{s}\big)/2$.

The above example creates entanglement deterministically between the signal and the pump photons. In order to implement the phase gate, however, it is necessary to ensure that these photons do not entangle at the cavity output. To this end, we propose to use photons in exponentially rising pulses whose temporal shapes replicate the "time reversed" cavity leakage modes [23]. This allows the entire pulse of the pump photon to be in the cavity when the signal photon arrives, so that the latter's phase is switched with certainty. Using such photons, we next simulate the switching dynamics in the CQZ case, taking $Q^\mathrm{c}_{\mathrm{p,f}} = 10^8$, $Q^\mathrm{c}_\mathrm{s} = 10^7$, and assuming all other parameters to be the same as in the Gaussian-pulse case considered above. The smaller Q^c_s results in a narrower signal pulse, which allows us to arrange the temporal delay of the signal photon relative to the pump to be such that it passes through the cavity when almost the entire pump pulse is already in the cavity. The simulation results are shown in Fig. 4, where plot 4(a) shows the signal input and output with the pump OFF. Except for the π phase shift, the temporal profile of the signal output is reversed indicating that the signal photon coupled into the cavity and then out. Figure 4(b) shows the signal input and the first Schmidt eigenfunction of the gate output with the pump ON. This first eigenfunction matches the input pulse shape very well and the fidelity reaches 0.99. The probability for the output signal photon to occupy this eigenmode is 0.98. Figure 4(c) shows the pump input and output with the signal OFF. The pulse evolution is similar to the signal's in the pump-OFF case. Figure 4(d) plots the pump input and the first Schmidt eigenfunction of the output with the signal ON. As shown, the pump photon couples into disk and then exits as if the signal photon did not exist. Both Figs. 4(a) and 4(c) show that the pulses start to leak out only after they have been entirely coupled in.

We further investigate the gate performance with larger disk sizes, which lead to a range of smaller Υ values (cf. Fig. 2). Both the fidelity and the probability of occupying the first Schmidt eigenmode are calculated and plotted in Fig. 5. Both plots show a saturation feature as Υ increases. This feature points to the feasibility of future experiments. As long as the disk radius is smaller than 25 µm, good single-photon switching performance can be expected.

In summary, we have proposed the use of the quantum Zeno blockade to achieve a large effective nonlinearity at the single-photon level. By performing a multimode analysis and considering realistically achievable parameters, we have shown that a deterministic phase gate can be implemented between single photons with near-ideal fidelity.

We acknowledge D. V. Strekalov and A. S. Kowligy for helpful discussions. This research was supported in part by the National Science Foundation (Grant No. ECCS-1232022), by the Defense Advanced Research Projects Agency (DARPA) under the Zeno-based Opto-

Electronics (ZOE) program (Grant No. W31P4Q-09-1-0014), and by the United States Air Force Office of Scientific Research (USAFOSR) (Grant No. FA9550-09-1-0593).

* yphuangpx@gmail.com

[1] P. A. Franken, A. E. Hill, C. W. Peters, and G. Weinreich, Phys. Rev. Lett. **7**, 118 (1961).

[2] N. P. Georgiades, E. S. Polzik, K. Edamatsu, H. J. Kimble, and A. S. Parkins, Phys. Rev. Lett. **75**, 3426 (1995).

[3] Y. Guo, P. P. Ho, H. Savage, D. Harris, P. Sacks, S. Schantz, F. Liu, N. Zhadin, and R. R. Alfano, Opt. Lett. **22**, 1323 (1997).

[4] R. Horodecki, P. Horodecki, M. Horodecki, and K. Horodecki, Rev. Mod. Phys. **81**, 865 (2009).

[5] D. A. B. Miller, Nature Photonics **4**, 3 (2010).

[6] M. A. Nielsen and I. L. Chuang, *Quantum Computation and Quantum Information* (Cambridge University Press, 2000).

[7] N. Sangouard, B. Sanguinetti, N. Curtz, N. Gisin, R. Thew, and H. Zbinden, Phys. Rev. Lett. **106**, 120403 (2011).

[8] N. K. Langford, S. Ramelow, R. Prevedel, W. J. Munro, G. J. Milburn, and A. Zeilinger, Nature **478**, 360 (2011).

[9] K. M. Birnbaum, A. Boca, R. Miller, A. D. Boozer, T. E. Northup, and H. J. Kimble, Nature **436**, 87 (2005).

[10] T. Volz, A. Reinhard, M. Winger, A. Badolato, K. J. Hennessy, E. L. Hu, and A. Imamoğlu, Nature Photonics **6**, 605 (2012).

[11] E. Knill, R. Laflamme, and G. J. Milburn, Nature **409**, 46 (2001).

[12] R. Raussendorf and H. J. Briegel, Phys. Rev. Lett. **86**, 5188 (2001).

[13] I. L. Chuang and Y. Yamamoto, Phys. Rev. A **52**, 3489 (1995).

[14] M. D. Lukin and A. Imamoğlu, Phys. Rev. Lett. **84**, 1419 (2000).

[15] Z.-B. Wang, K.-P. Marzlin, and B. C. Sanders, Phys. Rev. Lett. **97**, 063901 (2006).

[16] J. H. Shapiro, Phys. Rev. A **73**, 062305 (2006).

[17] J. Gea-Banacloche, Phys. Rev. A **81**, 043823 (2010).

[18] B. Misra and E. C. G. Sudarshan, Journal of Mathematical Physics **18**, 756 (1977).

[19] Y.-P. Huang and P. Kumar, Phys. Rev. Lett. **108**, 030502 (2012).

[20] Y. Huang and P. Kumar, Opt. Lett. **35**, 2376 (2010).

[21] Y.-P. Huang and P. Kumar, Selected Topics in Quantum Electronics, IEEE Journal of **18**, 600 (2012).

[22] Y. P. Huang and M. G. Moore, Phys. Rev. A **77**, 062332 (2008).

[23] J. I. Cirac, P. Zoller, H. J. Kimble, and H. Mabuchi, Phys. Rev. Lett. **78**, 3221 (1997).

[24] Y.-P. Huang, J. B. Altepeter, and P. Kumar, Phys. Rev. A **82**, 063826 (2010).

[25] J. D. Franson, B. C. Jacobs, and T. B. Pittman, Phys. Rev. A **70**, 062302 (2004).

[26] S. H. Autler and C. H. Townes, Phys. Rev. **100**, 703 (1955).

[27] Supplementary material: 1. Whispering Gallery Modes; 2. Calculation for Υ and the Data Plotted in Fig. 2; 3. IQZ Case Analysis.

[28] V. S. Ilchenko, A. A. Savchenkov, A. B. Matsko, and L. Maleki, Phys. Rev. Lett. **92**, 043903 (2004).

[29] J.-T. Shen and S. Fan, Phys. Rev. A **79**, 023838 (2009).

[30] Private communications with D. V. Strekalov.

[31] J. E. Heebner, T. C. Bond, and J. S. Kallman, Opt. Express **15**, 4452 (2007).

[32] S. M. Spillane, T. J. Kippenberg, K. J. Vahala, K. W. Goh, E. Wilcut, and H. J. Kimble, Phys. Rev. A **71**, 013817 (2005).

[33] J. U. Fürst, D. V. Strekalov, D. Elser, A. Aiello, U. L. Andersen, C. Marquardt, and G. Leuchs, Phys. Rev. Lett. **105**, 263904 (2010).

[34] J. Schwesyg, *Interaction of light with impurities in lithium niobate crystals*, Ph.D. thesis, Rheinischen Friedrich-Wilhelms-Universität Bonn (2011).

[35] I. Marcikic, H. de Riedmatten, W. Tittel, H. Zbinden and N. Gisin, Nature **421**, 509 (2003)

[36] W. Tittle, J. Brendel, H. Zbinden, and N. Gisin, Phys. Rev. Lett. **84**, 4737 (2000)